

Formation of low friction and wear-resistant carbon coatings on tool steel by 75 keV, high-dose carbon ion implantation

N. J. Mikkelsen, S. S. Eskildsen and C. A. Straede

Danish Technological Institute, Tooling and Process Engineering Department, Tribology Centre, Teknologiparken, DK-8000 Aarhus C (Denmark)

N. G. Chechenin

Institute of Physics and Astronomy, University of Aarhus, DK-8000 Aarhus C (Denmark)

Abstract

Hardened AISI D2 steel samples were subjected to mass-separated C^+ ion bombardment at 75 keV with ion doses in the range $0.5\text{--}15 \times 10^{18} C^+ cm^{-2}$. It was observed that sputtering was still limited, and the system exhibited internal growth, because most of the ions penetrated more than $0.1 \mu m$ into the growing carbon film. At the lowest ion doses applied, carbon was implanted into the steel, while higher doses resulted in the implanted carbon concentration near the surface being almost 100%. For the highest doses applied, Rutherford backscattering spectrometry and surface profilometry analyses showed that layers about $0.5\text{--}1 \mu m$ thick of almost pure carbon grew outward from the steel substrate. Transmission electron microscopy showed that the carbon layers were amorphous and exhibited an intermixed layer–substrate interface. The layers were hard and exhibited pronounced elastic recovery when subjected to ultralow load indentation. Low friction and excellent wear properties were measured when tested under dry conditions with a ball-on-disc tribometer.

1. Introduction

Several attempts have been made to deposit hard, wear-resistant carbon coatings—often designated “diamond-like coatings”, “DLCs”, “amorphous carbon” or “a-C”—on various substrates by low energy carbon ion (C^+) bombardment techniques with energies of about a few hundred electronvolts. With such approaches, the near surface, *i.e.* a few nanometres of the growing carbon layer, is continuously subjected to implantation of energetic carbon ions. The processes are non-thermal and can synthesize metastable phases, such as amorphous carbon, diamond or diamond-like carbon, on substrates at low temperatures [1, 2].

An increase in the ion energy to a few kiloelectronvolts enhances the sputtering rate and reduces the net film growth rate. Even inhibition of film growth has been observed at about 1 keV [3]. In addition, it is generally considered that the increase in ion energy into the kiloelectronvolt range results in implantation far into the substrate and not deposition on the surface, at least for relatively low ion doses. Thus, until now, most of the work has been made at carbon ion energies of less than a few kiloelectronvolts. However, to enhance the carbon layer adhesion and to create harder carbon phases, several investigators have introduced additional energy to the system by additional ion bombardment, either during the carbon deposition, by ion-beam-assisted deposition (IBAD) processes, or after deposition [2].

However, other results indicate that it may be possible to deposit almost pure carbon layers at higher energies. Thus, net outward surface growth of diamond by 100 keV C^+ implantation of diamond has been observed [4], and carbonaceous layers on CaF_2 have been obtained by 2–10 keV C^+ bombardment [5]. Epitaxial growth of thin diamond layers was observed [6, 7] when f.c.c. metals (such as copper), which have only a small crystal lattice mismatch with that of diamond, were bombarded with C^+ ions at energies of about 120 keV and at elevated temperatures. When steel is subjected to C^+ implantations at energies from 75 to 150 keV and at doses in the range $1\text{--}3 \times 10^{18} C^+ cm^{-2}$, carbonaceous layers are obtained in the steel surface, exhibiting low friction and low wear [8–10].

In the present work, it is shown that implanting a tool steel with 75 keV C^+ ions at very high doses of more than $2 \times 10^{18} C^+ cm^{-2}$ results in outward growth of an almost pure carbon layer on the steel. The layers are hard, amorphous and diamond-like, and exhibit pronounced elastic recovery when subjected to nanoindentation. The layers have a graduated interfacial zone between the steel substrate and the carbon layer, and tribological tests show that the layers exhibit low friction and are wear resistant. No delamination of the layer from the substrate has been observed during testing, which indicates strong adhesion to the steel.

2. Experimental details

Hardened (about 60 ± 1 HRC) AISI D2—1.55% C, 0.3% Si, 0.3% Mn, 12.0% Cr, 0.8% Mo, 0.8% V and 84.25% Fe (all in weight per cent)—cold working tool steel discs have been implanted with carbon ions. Before implantation, the discs were mechanically polished to a roughness of $0.005 \mu\text{m}$ (R_a) and cleaned [10].

The discs were implanted in a Danfysik 1090-200 high current accelerator [11] especially designed for the treatment of tools. The C^+ implantation energy was 75 keV, and the doses were 0.5, 1.0, 2.0, 4.0, 8.0 and $15 \times 10^{18} \text{C}^+ \text{cm}^{-2}$. In all cases, the sample temperature during implantation was below 200°C and the beam current density was about $35 \mu\text{A cm}^{-2}$. The mass-separated ion beam was magnetically scanned over the samples and the chamber pressure was kept below about $2.5 \times 10^{-3} \text{Pa}$.

The stoichiometry and film thickness (in carbon atoms per square centimetre) were measured by Rutherford backscattering spectrometry (RBS), and the surface hardness of the samples was measured with a Nano-IndenterTMII. The film thickness, morphology and crystallinity were studied by scanning electron microscopy (SEM) and 200 keV transmission electron microscopy (TEM).

The discs were tested in a unidirectional ball-on-disc tribometer under unlubricated conditions, in a controlled environment of atmospheric air with relative humidity (RH) of $40 \pm 5\%$. A steel ball (AISI 52100, 5 mm in diameter) was made to slide over a total sliding distance of 1000 m at 0.1m s^{-1} , with a specified load of 2.4 N against the rotating disc. The wear track diameter was 20 mm [10].

In addition to the coefficients of friction, the area of the wear scar of the discs was measured by stylus profilometry [10]. The wear of the unimplanted counterpart, *i.e.* the ball, was measured by microscopy.

3. Results and discussion

3.1. Structure of the implanted steel

After implantation, most of the samples showed little visible change when compared with the unimplanted, mirror-like polished steel. When the implantation doses reach $4\text{--}8 \times 10^{18} \text{C}^+ \text{cm}^{-2}$, the samples began to reveal a minor change in colour towards a slightly bluish but clear appearance. The samples implanted at $15 \times 10^{18} \text{C}^+ \text{cm}^{-2}$ were markedly different. They exhibited a matt blackish appearance and could easily be scratched. The surface roughness (R_a value) was measured to be less than $0.009 \mu\text{m}$ for doses up to $8 \times 10^{18} \text{C}^+ \text{cm}^{-2}$, and about $0.08 \mu\text{m}$ for the $15 \times 10^{18} \text{C}^+ \text{cm}^{-2}$ dose.

SEM investigations show that the surface of the

samples implanted at doses lower than $8 \times 10^{18} \text{C}^+ \text{cm}^{-2}$ are smooth and have a dense morphology. The samples implanted at $15 \times 10^{18} \text{C}^+ \text{cm}^{-2}$ reveal a porous fibrous structure, probably causing the blackish appearance mentioned above. Furthermore, SEM investigations may indicate the presence of a few small pinholes in the surface, covering about 0.5% of the surface.

The profilometry scan in Fig. 1 shows that the implantation has added $0.56 \pm 0.2 \mu\text{m}$ to the surface of a sample implanted at $8 \times 10^{18} \text{C}^+ \text{cm}^{-2}$, clearly indicating outward growth of a surface layer. In Fig. 2 are shown RBS spectra of the steel samples implanted at 4×10^{18} and $8 \times 10^{18} \text{C}^+ \text{cm}^{-2}$. The presence of large amounts of carbon in the steel surface will result in a lack of backscattering yield from this steel when compared with the yield from pristine steel.

For the implantation at $4 \times 10^{18} \text{C}^+ \text{cm}^{-2}$, a surface peak from steel is observed, indicating the presence of iron and/or chromium at the surface. However, at larger depths, the yield from the iron and/or chromium is much lower, indicating a very high carbon content. For the implantation at $8 \times 10^{18} \text{C}^+ \text{cm}^{-2}$, the carbon layer is thicker and the steel surface peak is smaller. In addition, the carbon content in the layer is even higher when compared with that obtained at the lower dose. By comparing the fitted spectra (dashed lines) with the measured spectra, a broadened interface between the carbon layers and steel is clearly visible, indicating a mixed steel-carbon zone.

In Table 1 are shown the results of the RBS analysis of the steel implanted at the three highest doses. The retained doses, *i.e.* the thickness of the carbon layers in carbon atoms/per square centimetre, are comparable with the implanted dose, indicating a very low sputtering yield of the system. Layer thicknesses of 0.39, 0.70 and $1.2 \mu\text{m}$ are synthesized on the steel for the three higher doses respectively. They have a maximum carbon content between 97.6% and 99.4%, and a broad mixed carbon layer-steel interface extending to about $0.15 \mu\text{m}$ for the two lower doses and apparently $0.48 \mu\text{m}$ for the highest dose.

The results of the RBS measurements are confirmed by TEM cross-section measurements of a steel sample implanted at $4 \times 10^{18} \text{C}^+ \text{cm}^{-2}$ (Fig. 3). A well-defined surface layer on the steel substrate is seen, with a graduated interface between the carbon and steel. The mean layer thickness from the surface to the middle of the interface is $0.34 \pm 0.03 \mu\text{m}$, giving a carbon phase mass density of $2.6 \pm 0.4 \text{g cm}^{-3}$, and the extension of the interface is about $0.14 \mu\text{m}$. Electron diffraction analyses show that the surface layer is amorphous carbon and that the interface consists of a mixed zone of crystalline steel with an increasing amount of amorphous carbon towards the surface. At the surface of the carbon layer, very small (less than 5 nm) precipitates containing iron and chromium are identified.

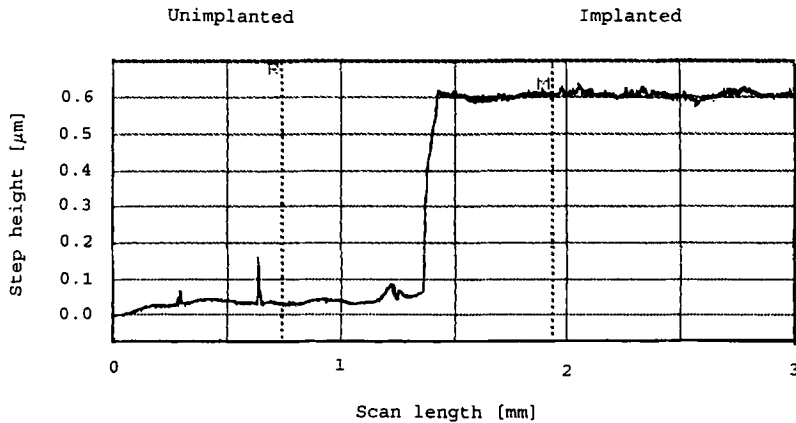


Fig. 1. Stylus profilometry scan of a D2 steel surface implanted with $8 \times 10^{18} \text{ C}^+ \text{ cm}^{-2}$ at 75 keV.

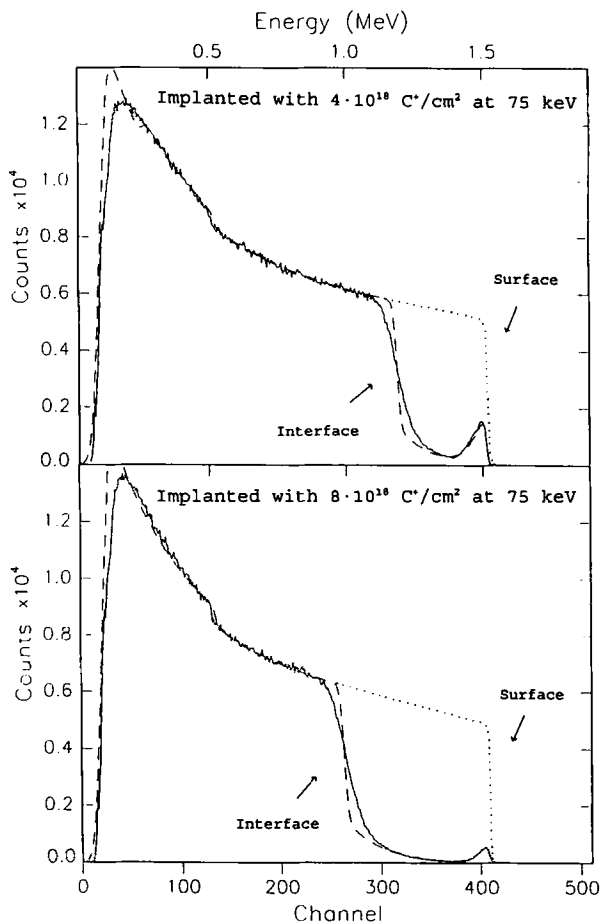


Fig. 2. RBS spectra of high dose carbon-implanted D2 steel: —, experimental spectra; ..., simulated spectra of unimplanted steel; ---, simulated spectra of carbon layers with varying amounts of steel content, fitted to the experimental spectra. The simulated fitted spectra are made under the assumption that the interface between the carbon layer and the steel is abrupt.

3.2. Mechanical and tribological properties

In Fig. 4 are shown typical loading–unloading nanoindentation curves for an unimplanted hardened D2 steel sample compared with a steel sample implanted with

$8 \times 10^{18} \text{ C}^+ \text{ cm}^{-2}$. The nanoindentations were performed at depths from 0.07 to 0.25 μm and the average hardness of the unimplanted sample was $12.3 \pm 3.5 \text{ GPa}$. For samples implanted at 4×10^{18} and $8 \times 10^{18} \text{ C}^+ \text{ cm}^{-2}$, the hardnesses were 11.4 ± 0.8 and $11.6 \pm 1.4 \text{ GPa}$, respectively, *i.e.* very similar to the hardness of the unimplanted steel and to nanoindentation measurements on DLCs made by r.f. glow discharge systems [12]. For samples implanted at $15 \times 10^{18} \text{ C}^+ \text{ cm}^{-2}$, no conclusive data could be given, as a result of their porous and fragile structure.

When studying the unloading part of the curves in Fig. 4, it is clearly seen that the residual indentation depths, *i.e.* at zero load, for the carbon-implanted sample are about two times smaller than those of the unimplanted steel, indicating a marked elastic recovery of the carbon layers. Thus, if hardness measurements were made by traditional methods where the indentation depths were determined by microscopy inspection of the residual indentation marks, the measured hardness of the steel sample implanted at $8 \times 10^{18} \text{ C}^+ \text{ cm}^{-2}$ would be about four times that of the unimplanted sample, *i.e.* about 50 GPa. These observations are similar to those made from studies on DLCs by plasma-enhanced chemical vapour deposition, where nanoindentation measurements gave hardness values from 5 to 15 GPa, whereas Knoop measurements, in comparison, revealed hardness values 3–4 times higher than that [13].

In Fig. 5 are shown the results of the tribological investigations made with the ball-on-disc tester. Figure 5(a) clearly shows that carbon implantation reduces the coefficient of friction, even at the lower doses [8–10]. The lowest coefficient of friction, *i.e.* about 0.22–0.3, is observed at doses of 1, 2 and $4 \times 10^{18} \text{ C}^+ \text{ cm}^{-2}$. These values are comparable with values measured on ion-beam-deposited DLC layers on a hardened steel at a low energy [14]. The dose of $1 \times 10^{18} \text{ C}^+ \text{ cm}^{-2}$ results in the lowest value. However, as a result of the uncertainty of the data, this may not

TABLE 1. Carbon surface layer thicknesses, carbon concentrations and the extension of the interface of high dose carbon ion-implanted D2 steel, as measured by RBS

Implanted ion dose ($\times 10^{18} \text{ C}^+ \text{ cm}^{-2}$)	Thickness of implanted carbon layer ($\times 10^{18} \text{ C cm}^{-2}$)	Calculated geometrical thickness ^a (μm)	Surface carbon concentration (at.%)	Maximum carbon concentration (at.%)	Extension of the interface zone (μm)
4.0 ± 0.8	4.4 ± 0.5	0.39 ± 0.04	79	97.6	≈ 0.15
8.0 ± 1.6	7.9 ± 1.0	0.70 ± 0.09	93	99.4 ^b	≈ 0.15
15 ± 3	13 ± 2	1.2 ± 0.2	99.4 ^b	99.4 ^b	$\approx 0.48^c$

^aThe values have been calculated by assuming a carbon mass density of 2.3 g cm^{-3} .

^bThe value of 99.4% can be explained by a possible presence of small holes in the layers, covering about 0.5% of the layers. Thus, the real carbon concentration may be 100%.

^cThis value may be too high, as a result of surface roughness and a porous structure. The real value may be lower, and is probably about $0.15 \mu\text{m}$.

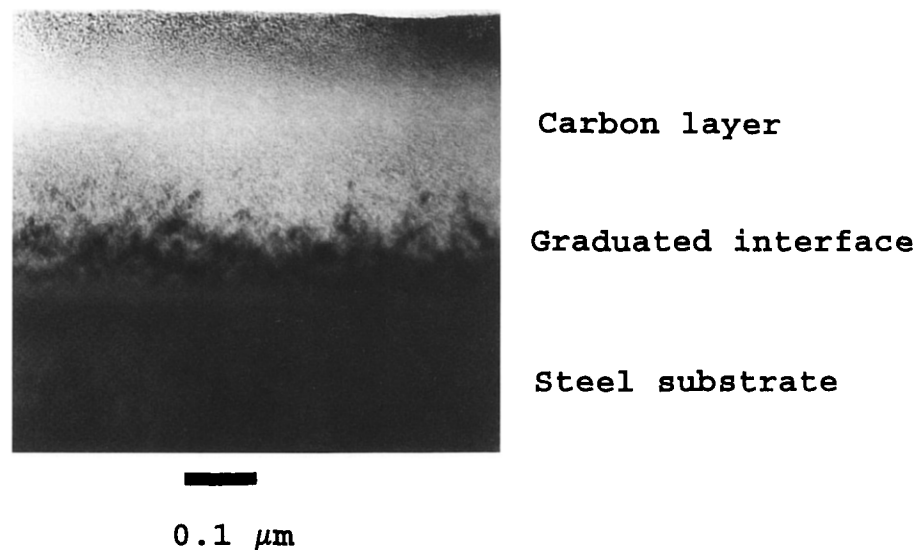


Fig. 3. Bright-field TEM cross-sectional micrograph of a D2 steel sample implanted with $4 \times 10^{18} \text{ C}^+ \text{ cm}^{-2}$ at 75 keV. The geometrical thickness of the layer is $0.34 \pm 0.3 \mu\text{m}$, indicating a mass density of about $2.6 \pm 0.4 \text{ g cm}^{-3}$.

be conclusive. Furthermore, it is evident that, at higher doses, *i.e.* 8×10^{18} and $15 \times 10^{18} \text{ C}^+ \text{ cm}^{-2}$, the friction increases when the dose is increased, reaching about 0.8 for the higher dose.

The wear of the implanted disc (Fig. 5(b)) and that of the unimplanted ball (Fig. 5(c)) are lowest at $4 \times 10^{18} \text{ C}^+ \text{ cm}^{-2}$. At this dose, the wear of the implanted disc is eight times smaller than the mean wear value of the unimplanted discs, and the wear of the ball is 3.7×10^4 times smaller than that for a ball slid against an unimplanted disc. The wear of the unimplanted discs varies between positive wear, *i.e.* adhesion of ball material to the disc, and negative wear, *i.e.* removal of disc material. This is reflected by the large error bar shown in the figure. For the carbon-implanted samples, no adhesion of ball material was observed, and the scatter of the wear data was orders of magnitude less than that for the unimplanted disc. In all the tests performed, no

delamination of the layers from the substrate was observed, indicating strong layer-substrate adhesion.

A clear trend showing increasing friction and wear for doses above $4 \times 10^{18} \text{ C}^+ \text{ cm}^{-2}$ is observed. The increasing wear of the disc may be explained by an increasing loss of cohesiveness of the layer. The increasing friction and enhanced wear of the ball may result from increasing amounts of hard abrasive particles incorporated into the coating. At the highest dose, the cohesiveness of the carbon coating may be eliminated, yielding very high disc wear and inhibiting proper nanoindentation measurements. However, TEM investigations of these samples show that the layer consists of pure amorphous carbon.

4. Conclusions

Implantations of 75 keV C^+ ions into hardened D2 steel at doses from 1×10^{18} to $8 \times 10^{18} \text{ C}^+ \text{ cm}^{-2}$ result

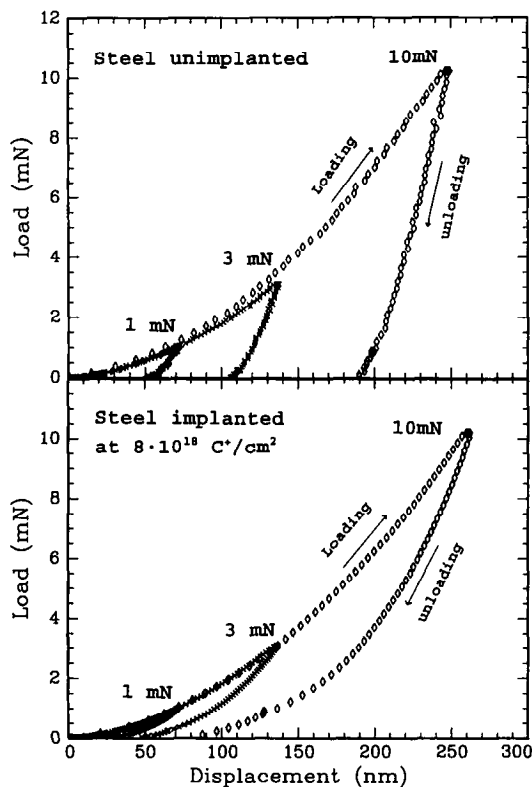


Fig. 4. Typical loading-unloading curves for nanoindentations of unimplanted D2 steel compared with D2 steel implanted with a high dose of 75 keV C^+ ions. The hardness has been extrapolated, using a linear fit to the top part of the unloading curves.

in the formation of low friction, wear-resistant carbonaceous surface layers. At very high doses, *i.e.* 4, 8 and $15 \times 10^{18} C^+ cm^{-2}$, almost 100% pure carbon layers are synthesized on the steel, having thicknesses proportional to the ion dose and ranging from 0.39 to 1.2 μm . The layers are amorphous, apparently diamond-like and adhere well to the substrate, owing to a graduated interfacial zone 0.15 μm thick. As a result of the relatively high ion energy applied in this study, most of the carbon ions are continuously deposited deep into the growing layer, *i.e.* more than 0.1 μm . Thus, the layers are synthesized by internal growth and, during growth, significant amounts of energy are deposited by the bombarding ions, *i.e.* the system acts as an IBAD process and has the advantages of this technique. However, in the present approach, the additional ion bombardment is incorporated into the process.

Under the present implantation and test conditions, the optimum dose to obtain minimum wear is $4 \times 10^{18} C^+ cm^{-2}$. However, low friction is achievable at lower doses, down to $1 \times 10^{18} C^+ cm^{-2}$. The layers implanted at 4 and $8 \times 10^{18} C^+ cm^{-2}$ have hardness values of about 12 GPa, when measured by nanoindentation. However, more conventional microhardness measurements would reveal hardnesses of the order of

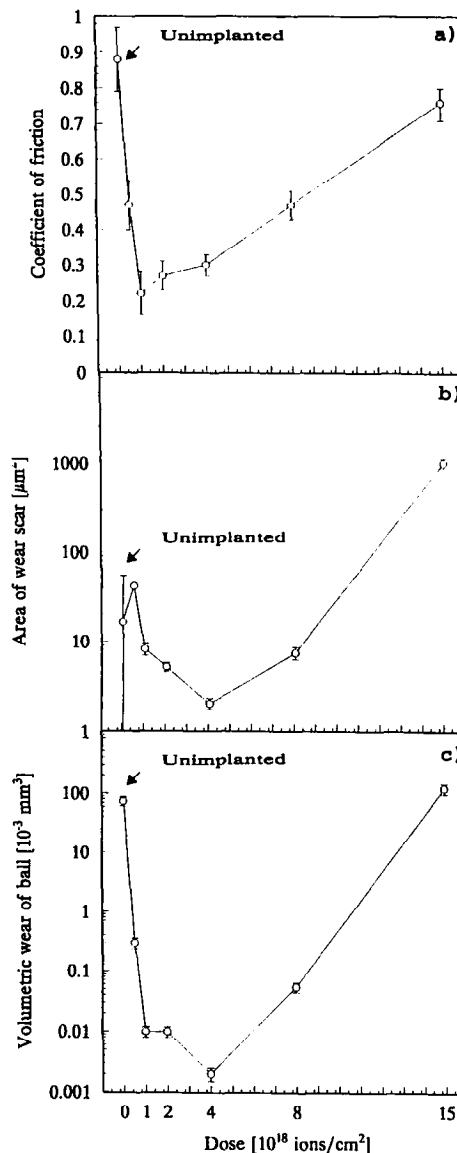


Fig. 5. Friction and wear measurements of hardened D2 steel discs implanted with 75 keV C^+ ions at doses from 0.5×10^{18} to $15 \times 10^{18} C^+ cm^{-2}$. The tests were made under unlubricated conditions on a ball-on-disc tribometer.

50 GPa. At $15 \times 10^{18} C^+ cm^{-2}$, the layer acts as a non-cohesive coating with abrasive particles incorporated. This may result from radiation damage or local stress fields when implanting at extremely high doses, causing the formation of small domains of very hard amorphous carbon phases.

The present layers were made at ion doses about one order of magnitude larger than those normally applied in commercial ion implantation of tools and components. Thus, with the present techniques available, these coatings are quite expensive. However, the ion implantation technique is rapidly developing. Indeed, the present results have shown that the method is feasible and that, by further studies and developments, highly adherent

and superior DLC coatings may be applied on a variety of substrates at low deposition temperatures.

Acknowledgments

The help of J. Chevallier (TEM investigations), and J. P. Krogh (RBS measurements), Institute of Physics and Astronomy, University of Aarhus, Denmark is greatly acknowledged. The work has been supported by the Danish Materials Technology Development Programme, Centre for Surface Technology—Dry Coating Processes.

References

- 1 J.-P. Hirvonen, J. Koskinen, R. Lappalainen, A. Anttila and M. Trkula, *J. Electron. Mater.*, 20 (1991) 127.
- 2 S. Aisenberg and F. M. Kimock, *Mater. Sci. Forum*, 52–53 (1990) 1.
- 3 R. Wei, P. J. Wilbur, A. Erdemir and F. M. Kustas, *Surf. Coat. Technol.*, 51 (1992) 139.
- 4 R. S. Nelson, J. A. Hudson, D. J. Mazey and R. C. Pillar, *Proc. R. Soc. London, Ser. A*, 386 (1983) 211.
- 5 M. L. Stein, S. Aisenberg and B. Bendow, in H. E. Bennett et al. (eds.), *Laser Induced Damage in Optical Materials: 1981*, ASTM Spec. Tech. Publ., 799, (1983) 482.
- 6 J. F. Prins, *US Patent*, 4,997,636, 1991.
- 7 H. A. Hoff, D. J. Vestyck, Jr., J. E. Butler and J. F. Prins, *Appl. Phys. Lett.*, 62 (1) (1993) 34.
- 8 K. Kobs, H. Dimigen, C. J. M. Denissen, E. Gerritsen, J. Politiek, L. J. van Ijzendoorn, R. Oechsner, A. Kluge and H. Ryssel, *Appl. Phys. Lett.*, 57 (1990) 1622.
- 9 C. A. Straede, J. R. Poulsen, B. M. Lund and G. Sørensen, *Mater. Sci. Eng.*, A139 (1991) 150.
- 10 N. J. Mikkelsen and C. A. Straede, *Surf. Coat. Technol.*, 51 (1992) 152.
- 11 B. R. Nielsen, P. Abrahamsen and S. Eriksen, *Mater. Sci. Eng.*, A116 (1989) 193.
- 12 D. L. Joslin, M. E. O'Hern, C. J. McHargue, R. E. Clausing and W. C. Oliver, *Proc. SPIE*, 1050 (1989) 218.
- 13 X. Jiang, K. Reichelt and B. Stritzker, *J. Appl. Phys.*, 66 (1989) 5805.
- 14 F. M. Kustas, M. S. Misra, D. F. Shepard and J. F. Froechtenigt, *Surf. Coat. Technol.*, 48 (1991) 113.